

RESEARCH

Open Access



Targeting deubiquitinase USP7-mediated stabilization of XPO1 contributes to the anti-myeloma effects of selinexor

Junying Wang¹, Mengping Chen¹, Jinxing Jiang¹, Yike Wan¹, Xin Li¹, Minyue Zhang¹, Fei Xiao¹, Lu Zhong^{1,2}, Hua Zhong¹, Zhaoyu Qin^{3*} and Jian Hou^{1*} 

Abstract

Background Targeting exportin1 (XPO1) with Selinexor (SEL) is a promising therapeutic strategy for patients with multiple myeloma (MM). However, intrinsic and acquired drug resistance constitute great challenges. SEL has been reported to promote the degradation of XPO1 protein in tumor cells. Nevertheless, in myeloma, the precise mechanisms underlying SEL-induced XPO1 degradation and its impact on drug responsiveness remain largely undefined.

Methods We assessed XPO1 protein and mRNA levels using western blotting and RT-qPCR. Cycloheximide (CHX) chase assays and degradation blockade assays were used to determine the pathway of XPO1 degradation induced by SEL. The sensitivity of MM cell lines to SEL was evaluated using CCK8-based cell viability assays and AV-PI staining-based cell apoptosis assays. The subcellular localization of the cargo protein RanBP1 was assessed via immunofluorescence staining. Immunoprecipitation coupled with mass spectrometry (IP-MS), bioinformatics analysis and ubiquitination assays, were employed to identify the molecular targets responsible for SEL-induced degradation of XPO1. shRNA-mediated knockdown assays and small molecule inhibitors of USP7 were utilized to disrupt the function of USP7. The role of USP7 in modulating SEL sensitivity was analyzed in MM cell lines, primary CD138⁺ cells, and xenograft mouse models.

Results SEL promotes the degradation of XPO1 in MM cells through the ubiquitin–proteasome pathway. There is a positive correlation between XPO1 degradation and sensitivity to SEL in these cells. Inhibiting XPO1 degradation reduces the functional inhibitory effects of SEL on XPO1, as evidenced by decreased nuclear localization of the cargo protein RanBP1. USP7 stabilizes XPO1 in MM cells via its deubiquitinating activity. SEL accelerates the ubiquitination and subsequent degradation of XPO1 by disrupting the interaction between XPO1 and USP7. The expression of USP7 is negatively correlated with patient prognosis and the sensitivity of MM cells to SEL. Inactivating or knocking down USP7 significantly enhances the anti-myeloma effects of SEL both in vitro and in vivo.

Conclusion In conclusion, our findings underscore the essential role of XPO1 degradation in the anti-myeloma efficacy of SEL and establish a research foundation for targeting USP7 to improve the effectiveness of SEL-based therapies in MM.

Keywords Multiple myeloma, Selinexor, XPO1, USP7, Protein degradation, Drug sensitivity

*Correspondence:

Zhaoyu Qin
qinzhaoyu@fudan.edu.cn
Jian Hou
houjian@medmail.com.cn

Full list of author information is available at the end of the article



© The Author(s) 2025. **Open Access** This article is licensed under a Creative Commons Attribution-NonCommercial-NoDerivatives 4.0 International License, which permits any non-commercial use, sharing, distribution and reproduction in any medium or format, as long as you give appropriate credit to the original author(s) and the source, provide a link to the Creative Commons licence, and indicate if you modified the licensed material. You do not have permission under this licence to share adapted material derived from this article or parts of it. The images or other third party material in this article are included in the article's Creative Commons licence, unless indicated otherwise in a credit line to the material. If material is not included in the article's Creative Commons licence and your intended use is not permitted by statutory regulation or exceeds the permitted use, you will need to obtain permission directly from the copyright holder. To view a copy of this licence, visit <http://creativecommons.org/licenses/by-nc-nd/4.0/>.

Background

Multiple myeloma (MM) is the second most commonly diagnosed hematologic malignancy, characterized by abnormal proliferation of clonal plasma cells in the bone marrow [1]. Despite significant progress has been made in the treatment of myeloma, inherent and acquired drug resistance remains a major limitation for long-term disease control [2, 3].

XPO1 is a nuclear export receptor that mediates the transport of cargo proteins bearing a nuclear export signal (NES), including various tumor suppressor proteins (TSPs) and growth regulatory proteins [4]. Through exporting several RNA-binding proteins and adaptor proteins, XPO1 is also responsible for transporting certain subsets of RNAs to the cytoplasm [5, 6]. XPO1 is frequently overexpressed and/or mutated in cancers and is considered as an oncogenic driver [7, 8]. Recently, several studies have highlighted the significant role of XPO1 in the progression and drug resistance of MM [8–10]. Consequently, targeting XPO1 has emerged as an attractive strategy for treating MM, particularly in relapsed/refractory patients [11].

Selinexor (SEL) is the first generation of selective inhibitors of nuclear export (SINE) that has been approved for RRMM in 2019 [12]. SEL covalently binds into the cargo-binding cleft of XPO1, locking TSPs in the nucleus and resulting in proliferation inhibition and apoptosis of cancer cells [9]. SEL performs well when used in combination with other established drugs such as dexamethasone, proteasome inhibitors, and immunomodulators [13, 14]. Nonetheless, therapeutic responses to SEL exhibit considerable variability among patients. The mechanism through which SEL impedes myeloma progression remains largely to be determined, as do the indicative biomarkers for responses to XPO1-targeted therapy [7]. A thorough understanding of the drug's mechanisms of action could provide invaluable insights to augment the efficacy of SEL-based therapies.

Previous studies have indicated that SEL disrupts the docking of cargoes to XPO1, thereby blocking its nuclear export [15]. Moreover, several recent investigations have revealed that SEL facilitates the degradation of XPO1 protein in tumor cells [16]. Kwanten et al. reported that E3 ubiquitin ligase ASB8 can promote SEL-induced degradation of XPO1 [17]. However, functional experiments in their study demonstrated that both ASB8 knockout and overexpression rendered cells more sensitive to SEL. This paradoxical finding suggests that ASB8 alone cannot sufficiently explain the variability in patient sensitivity to SEL, indicating that other mechanisms may also be involved.

Considering that reductions of XPO1 protein levels can significantly influence its overall functionality, we

propose that this mechanism may be implicated in the anti-myeloma effects of SEL. Therefore, our study aims to investigate the role of XPO1 degradation in the anti-myeloma effects of SEL and to further elucidate the molecular mechanisms by which SEL induces XPO1 degradation in MM cells.

Materials and methods

Antibodies and reagents

Antibodies against the following proteins were purchased from Cell Signaling Technology: CRM1 (#46,249), USP7 (#4833), and Ubiquitin (#3936). Antibodies against the following proteins were purchased from Proteintech Technology: RanBP1 (27,804–1-AP), α -Tubulin (66,031–1-Ig), β -actin (66,009–1-Ig). Alexa Fluor[®] 488 Goat Anti-Rabbit IgG H&L (ab150077) was purchased from Abcam. SEL, Eltanexor (ELT), Verdinexor (VER), Cycloheximide (CHX), MG132 and Leupeptin (LEU) were purchased from Selleckchem (Munich, Germany).

Preparation of primary cell samples and cell culture

This study received approval from the Ethics Committee of Renji Hospital, affiliated with the Shanghai Jiao Tong University School of Medicine (Ethics Approval Number: KY2020-191). Primary CD138⁺ cells were isolated from bone marrow aspirates of three multiple myeloma patients after obtaining informed consent. Generally, bone marrow mononuclear cells were separated utilizing Ficoll density gradient sedimentation, followed by the isolation of CD138⁺ cells through microbead separation (Miltenyi, Germany). The detailed information of patients is listed in supplementary Table S1. CD138⁺ cells were cultured in RPMI-1640 medium (Hyclone, USA) containing 20% fetal bovine serum (Bovogen, Australia) and supplemented with 1% penicillin/streptomycin and 1% L-glutamine. Human multiple myeloma cell lines, including MM.1S, NCI-H929, U266 and RPMI-8226, were obtained from the American Type Culture Collection (ATCC) and have been cryopreserved at the Renji Blood Research Laboratory. MM cell lines were cultured in RPMI-1640 medium (Hyclone, USA) containing 10% fetal bovine serum (Bovogen, Australia) and supplemented with 1% penicillin/streptomycin and 1% L-glutamine. Cells were maintained at 37 °C with 5% CO₂ in humidified atmosphere.

Western blot

Total protein was extracted using RIPA lysis buffer (Beyotime, China). Proteins were electrophoresed by sodium dodecyl sulfate–polyacrylamide gel electrophoresis (SDS-PAGE) and subsequently transferred to a polyvinylidene fluoride membrane (Millipore, USA). Membranes were blocked with 5% BSA for 1 h and then

incubated with primary antibodies at 4 °C overnight. On the next day, membranes were incubated with a secondary antibody for 1 h and detected by enhanced chemiluminescence (Millipore, USA).

RNA extraction and RT-qPCR

RNA was extracted using RNeasy Mini Kit (Qiagen, Germany), followed by reverse transcription. Real-time quantitative PCR (RT-qPCR) was performed with ChamQ Universal SYBR qPCR Master Mix (Vazyme, China) according to the instruction manuals. qPCR standard protocol was 95 °C for 5 min, followed by 45 cycles of 95 °C for 10 s and 60 °C for 30 s. Expression fold change was calculated with $2^{-(\Delta\Delta C_t)}$. The primer sequences used in this study are listed in supplementary Table S2.

Cycloheximide (CHX)-chase assays

CHX-chase experiments were performed to detect the half-life of XPO1 protein. Briefly, MM cells under various treatment conditions were additionally treated with CHX (200 µg/mL) for the indicated times. After indicated time periods, the cell lysates were harvested and subjected to immunoblotting analysis of XPO1 protein levels.

Co-immunoprecipitation (Co-IP) assay

Immunoprecipitation was conducted using IP/Co-IP kit (Absin, China) in accordance with the manufacturer's instructions. Briefly, cell lysates from 5×10^7 cells were prepared with lysis buffer supplemented with protease inhibitors (Beyotime, China). Then, the lysates were incubated with primary either IgG or bait protein antibodies overnight at 4 °C. On the next day, 5 µL Protein A/G agarose beads were added to each sample and incubated at 4 °C on a rotator for another 3 h. Then, the beads were washed 3 times with 1 × wash buffer, proteins were eluted using 2 × loading buffer at 95 °C for 5 min. The proteins were then separated by SDS-PAGE. Then proteins in the immunoprecipitates were analyzed by western blot analysis.

Ubiquitination assays

To evaluate the ubiquitination level of endogenous XPO1, the cells were additionally treated with 10 µM MG132 for 6 h prior to collection. Subsequently, the cells were lysed and subjected to immunoprecipitation using anti-XPO1 antibody followed by SDS-PAGE. The ubiquitination of XPO1 was assessed utilizing the anti-ubiquitin antibody.

Cell viability assay

Cells (2×10^4 cells/well) were seeded in 96-well plates and treated with the indicated reagents for 48 h. Cell

viability assays were performed using Cell Counting Kit-8 (Dojindo, Japan) according to the manufacturer's instructions. Half-maximal inhibitory concentration (IC50) was determined using GraphPad Prism 8.0.

Cell apoptosis detection

To detect cell apoptosis, the cells were harvested and washed twice with PBS. Cells were then resuspended in 100 µL of 1 × binding buffer, followed by the addition of 5 µL of Annexin V-FITC (BD Biosciences, USA) and 5 µL of propidium iodide (PI) (BD Biosciences, USA). After 15 min of incubation in the dark, the samples were subjected to analysis via flow cytometry (Beckman Coulter, USA).

Immunofluorescent staining

Cellular smears were prepared using a cytospin centrifuge (Thermo Fisher Scientific, USA). Cells were fixed with 4% paraformaldehyde phosphate buffer solution (Beyotime, China) for 15 min. Cell membranes were permeabilized by Triton X-100 (Beyotime, China) for 15 min and blocked with 5% BSA for 1 h at room temperature. Subsequently, cells were incubated with primary anti-RanBP1 antibody overnight at 4 °C. On the next day, the sections were washed and subsequently incubated with Alexa Fluor® 488 Goat Anti-Rabbit IgG antibody for 1 h at room temperature. Cell nuclei were stained with DAPI (Beyotime, China). All images were acquired using a fluorescence microscope (Olympus BX51, Japan).

Immunoprecipitation coupled with Mass Spectrometry (IP-MS)

For IP-MS assay, NCI-H929 cells were treated with either 500 nM SEL or DMSO control for 6 h. Cell lysates were extracted as mentioned above. Then, the lysates in both groups were incubated with either isotype control IgG antibody (IgG-group) or primary anti-XPO1 antibody (IP-group) overnight at 4 °C. On the next day, 5 µL Protein A/G agarose beads were added to each sample and incubated at 4 °C on a rotator for another 3 h. Then, the beads were washed 3 times with 1 × wash buffer, proteins were eluted using 2 × loading buffer at 95 °C for 5 min. Then proteins were separated by SDS-PAGE. Gel bands were excised and digested with sequencing-grade trypsin (Promega, USA). The resulting peptides were analyzed using a LUMOS mass spectrometer (Thermo Fisher Scientific, USA). The relative abundance of proteins was calculated using the fraction of total (FOT) values. A fold change (FC) of (IP-group)/(IgG-group) ≥ 10 was used to identify the interacting proteins of XPO1.

Screen for targets responsible for SEL-induced degradation of XPO1

Three steps were employed to identify the targets responsible for SEL-induced XPO1 degradation. First, the interacting proteins of XPO1 in both the DMSO control group and the SEL-treated group were identified based on the IP-MS results. Second, potential ubiquitin ligases or deubiquitinases that could interact with XPO1 were predicted using Ubibrowser (http://ubibrowser.bio-it.cn/ubibrowser_v3/). Finally, the results from the above two analyses were intersected. Potential targets include: (1) deubiquitinases that interact with XPO1 in the control group but lose this interaction in the SEL-treated group; and (2) ubiquitin ligases that do not bind to XPO1 in the control group but do establish binding with XPO1 in the SEL-treated group.

USP7 shRNA knockdown assay

Lentiviral vector-mediated doxycycline (DOX)-inducible shRNA was constructed to knock down USP7 expression in MM cells. The target sequences for Tet-on-shUSP7 (1# and 2#) are listed in supplementary Table S3. MM cells were incubated with lentivirus particles for 48 h and then washed with fresh culture media. Infected cells were selected following a 3-day incubation in puromycin (5 µg/mL). For functional experiments, selected cells were further treated with doxycycline (1 µg/mL) for 2 days to induce the knockdown of USP7. The efficiency of the knockdown was validated through RT-qPCR and western blot analysis.

MM xenograft mouse model

All animal studies followed the procedures and protocols of the Animal Ethical Committee of Ren Ji Hospital, Shanghai Jiao Tong University School of Medicine. Six to eight-week-old female severe combined immunodeficient (SCID) mice were obtained from SPF (Beijing) Biotechnology for the study. Tet-on shUSP7-U266 myeloma cells (2×10^6) in 100 µL of PBS were injected subcutaneously. Once the average tumor size reached 100 mm³, the mice were randomly divided into four groups and

treated with PBS, DOX (0.25 mg/ml, administered via drinking water), SEL (10 mg/kg, administered via gavage), or a combination of DOX and SEL for the duration of the experiment. Tumor sizes were measured using calipers, and the volume was calculated using the formula $0.5 \times \text{width}^2 \times \text{length}$. On day 30, the mice were sacrificed, and the tumor tissues were harvested, weighed, and photographed.

Immunohistochemistry analysis

Tumor tissues were fixed with paraformaldehyde and embedded with paraffin. Slides were incubated with primary antibody against USP7 (1:100, Santa Cruz) or Ki67 (1:200, Proteintech) overnight at 4 °C. Subsequently, the slides were incubated with the secondary antibody at 37 °C for 45 min. Images were captured using a Leica DMI 6000B microscope. The proportion of positively stained cells was analyzed using ImageJ software.

Statistics

Statistical analysis was performed using Prism 8.0 (GraphPad Software, La Jolla, CA). All data are presented as mean ± SD of at least three independent experiments of technical triplicates unless specifically stated otherwise. Unpaired two-sided t-tests were used to compare two experimental groups, while one-way ANOVA tests were utilized for comparing three or more experimental groups. P values below 0.05 were considered statistically significant (* $p < 0.05$, ** $p < 0.01$, *** $p < 0.001$, and **** $p < 0.0001$).

Results

SEL promotes the degradation of XPO1 protein through the ubiquitin–proteasome pathway in MM cells

To confirm the effects of SEL on the degradation of XPO1 protein in MM cells, we first examined the expression levels of XPO1 protein and mRNA in NCI-H929 cells simultaneously following SEL treatment. As shown in Fig. 1A, B, SEL treatment led to a time- and dose-dependent reduction in the protein expression levels of XPO1, whereas the mRNA levels did not exhibit a

(See figure on next page.)

Fig. 1 SEL promotes the degradation of XPO1 protein through the ubiquitin–proteasome pathway in MM cells. **A** and **B** NCI-H929 cells were treated with 50–1000 nM SEL for 24 h (left) or 500 nM SEL at indicated time intervals (right), XPO1 protein (**A**) and mRNA (**B**) levels were analyzed by immunoblotting and RT-qPCR, respectively. **C** NCI-H929 cells treated with DMSO or 500 nM SEL, with 200 µg/ml CHX added to both groups. The levels of XPO1 protein were analyzed by immunoblotting at the specified time intervals. The half-life of XPO1 protein was determined by calculating the mean data of 3 independent replicates. **D** NCI-H929 cells were treated with either DMSO or 100 nM SEL, followed by the addition of either the proteasome inhibitor MG-132 (ranging from 1 to 10 µM) or the lysosomal inhibitor LEU (ranging from 10 to 100 µM). After 12 h, the levels of XPO1 protein were analyzed by immunoblotting. **E** NCI-H929 were treated with either DMSO or 100 nM SEL for 12 h, followed by an additional treatment with 10 µM MG132 for 6 h prior to collection. XPO1 was then immunoprecipitated with the anti-XPO1 antibody, ubiquitination levels of endogenous XPO1 protein were analyzed by immunoblotting using a ubiquitin antibody. The data are expressed as mean ± SD. * $p < 0.05$, ** $p < 0.01$, *** $p < 0.001$, and **** $p < 0.0001$

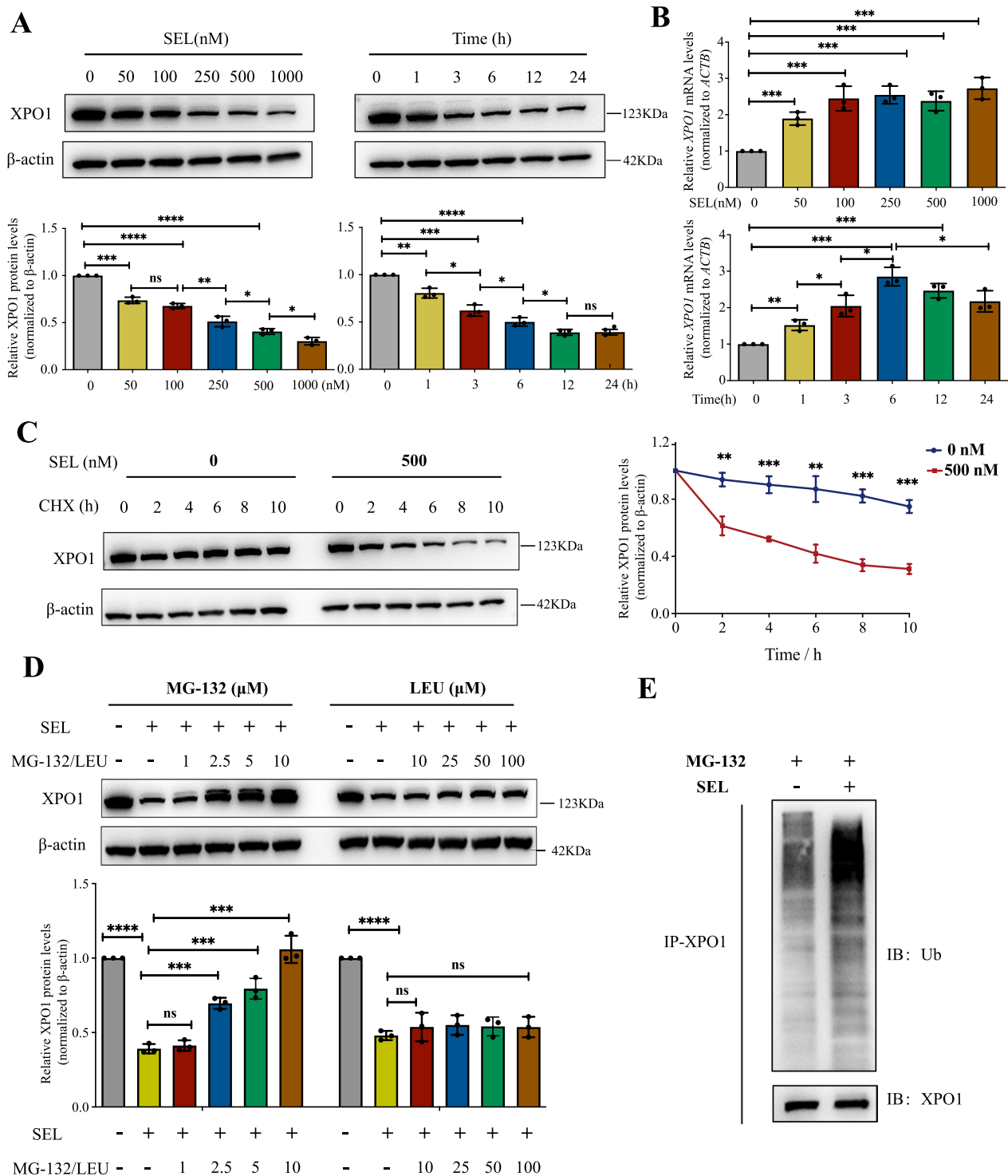


Fig. 1 (See legend on previous page.)

corresponding decline. In contrast, the mRNA levels of XPO1 increased following SEL treatment. These findings suggest that the reduction in XPO1 protein levels induced by SEL is not due to transcriptional repression.

To determine whether SEL promotes the degradation of XPO1 protein, we treated NCI-H929 cells with the protein synthesis inhibitor CHX, either alone or in

combination with SEL. As expected, SEL significantly accelerated the degradation rate of XPO1 in MM cells (Fig. 1C).

The ubiquitin proteasome pathway and the autophagy pathway serve as the primary mechanisms for protein degradation in eukaryotic cells [18]. To further elucidate the degradation pathway of XPO1 protein, we treated NCI-H929 cells with SEL in combination with either the ubiquitin proteasome inhibitors MG-132 or the autophagy/lysosome inhibitors Leupeptin (LEU). As illustrated in Fig. 1D, MG-132 effectively reversed the SEL-induced degradation of XPO1 in a dose-dependent manner. In contrast, LEU was unable to reverse the degradation of XPO1 induced by SEL, even at higher doses. We also validated these results in three additional MM cell lines. Consistent with our findings in NCI-H929 cells, proteasome inhibitors effectively reversed the protein reduction induced by SEL in MM.1S, U266, and RPMI-8226 cells, while lysosomal inhibitors showed no reversing effect (Supplementary Fig. S1). Subsequently, we analyzed the ubiquitination levels of endogenous XPO1. The results demonstrated a significant increase in the ubiquitination level of XPO1 following SEL treatment (Fig. 1E). Collectively, these results indicate that SEL facilitates the depletion of XPO1 in MM cells through ubiquitin-proteasomal-mediated degradation pathway.

The degradation of XPO1 protein exhibits a positive correlation with the sensitivity of MM cells to SEL treatment

To explore the potential role of XPO1 degradation in the anti-myeloma effects of SEL, we assessed the alterations in XPO1 protein levels following SEL treatment in MM cell lines with differing sensitivities to the drug. First, we evaluated the differences in the drug sensitivity among these MM cell lines. We performed a dose-dependent analysis of the inhibitory effects of SEL on a panel of MM cell lines, including NCI-H929, MM.1S, U266, and RPMI-8226. As shown in Fig. 2A, U266 and RPMI-8226 cells were less sensitive to SEL in terms of cell growth inhibition when compared to the other two cell lines. This was particularly evident in the significantly elevated IC₅₀ values observed in U266 and RPMI-8226 cells. Previous studies have also reported

similar findings, indicating that the IC₅₀ value of SEL is higher in U266 cells than in MM.1S cells [19, 20]. Furthermore, we assessed the differential sensitivity of these cell lines in response to two additional SINE compounds, specifically ELT and VER. As shown in Fig. 2B, C, the results were consistent with those observed for SEL. In addition, we examined the effects of SEL on cell apoptosis in these cell lines. As illustrated in Fig. 2D, cell apoptosis was more pronounced in NCI-H929 and MM.1S cells when exposed to the same concentration of SEL. These results suggest that U266 and RPMI-8226 cells exhibit a reduced sensitivity to SEL in comparison to MM.1S and NCI-H929 cells.

Subsequently, we evaluated XPO1 protein levels in these cell lines following SEL treatment. We found that, in accordance with the observed cytotoxic effects, the downregulation of XPO1 protein induced by SEL was more pronounced in NCI-H929 and MM.1S cells (Fig. 2E).

Based on these results, we hypothesize that the downregulation of XPO1 protein induced by SEL plays a crucial role in influencing drug sensitivity. To validate this hypothesis, we conducted additional analyses to determine whether the functional inhibition of XPO1 would be altered by blocking SEL-induced XPO1 degradation. Ran binding protein 1 (RanBP1) is a nuclear-cytoplasmic shuttling protein that is primarily enriched in the cytoplasm under standard culture conditions [21]. The nuclear accumulation of RanBP1 serves as a surrogate marker for XPO1 inhibition due to its widespread expression and rapid XPO1-dependent shuttling [22]. We analyzed the subcellular localization of RanBP1 following blocking XPO1 degradation by MG132. As illustrated in Fig. 2F–G, RanBP1 predominantly localized in the cytoplasm of cells treated with either DMSO or 10 μ M MG132. In contrast, SEL induced a significant accumulation of RanBP1 in the nucleus. However, co-treatment with SEL and MG132 resulted in a reduction of RanBP1's nuclear localization. These findings underscore the importance of XPO1 degradation in the efficacy of SEL.

(See figure on next page.)

Fig. 2 The degradation of XPO1 protein exhibits a positive correlation with the sensitivity of MM cells to SEL treatment. **A, B** and **C** Cell viability of MM cell lines treated with increasing concentrations of drugs for 48 h, and the IC₅₀ of SEL (**A**), ELT (**B**), VER (**C**) for each cell line. **D** Cell apoptosis rates of different MM cell lines after treated with indicated concentrations of SEL for 48 h. **E** Representative immunoblotting images and quantitative analysis of XPO1 protein levels in different MM cell lines treated with increasing concentrations of SEL for 24 h. **F** and **G** Immunofluorescent staining of RanBP1 (green) in NCI-H929 (**F**) and MM.1S (**G**) cells after treated with DMSO, MG132 (10 μ M) and /or SEL (500 nM) for 12 h. Nucleus were stained with DAPI (blue). The data are expressed as mean \pm SD. * p < 0.05, ** p < 0.01, *** p < 0.001, and **** p < 0.0001

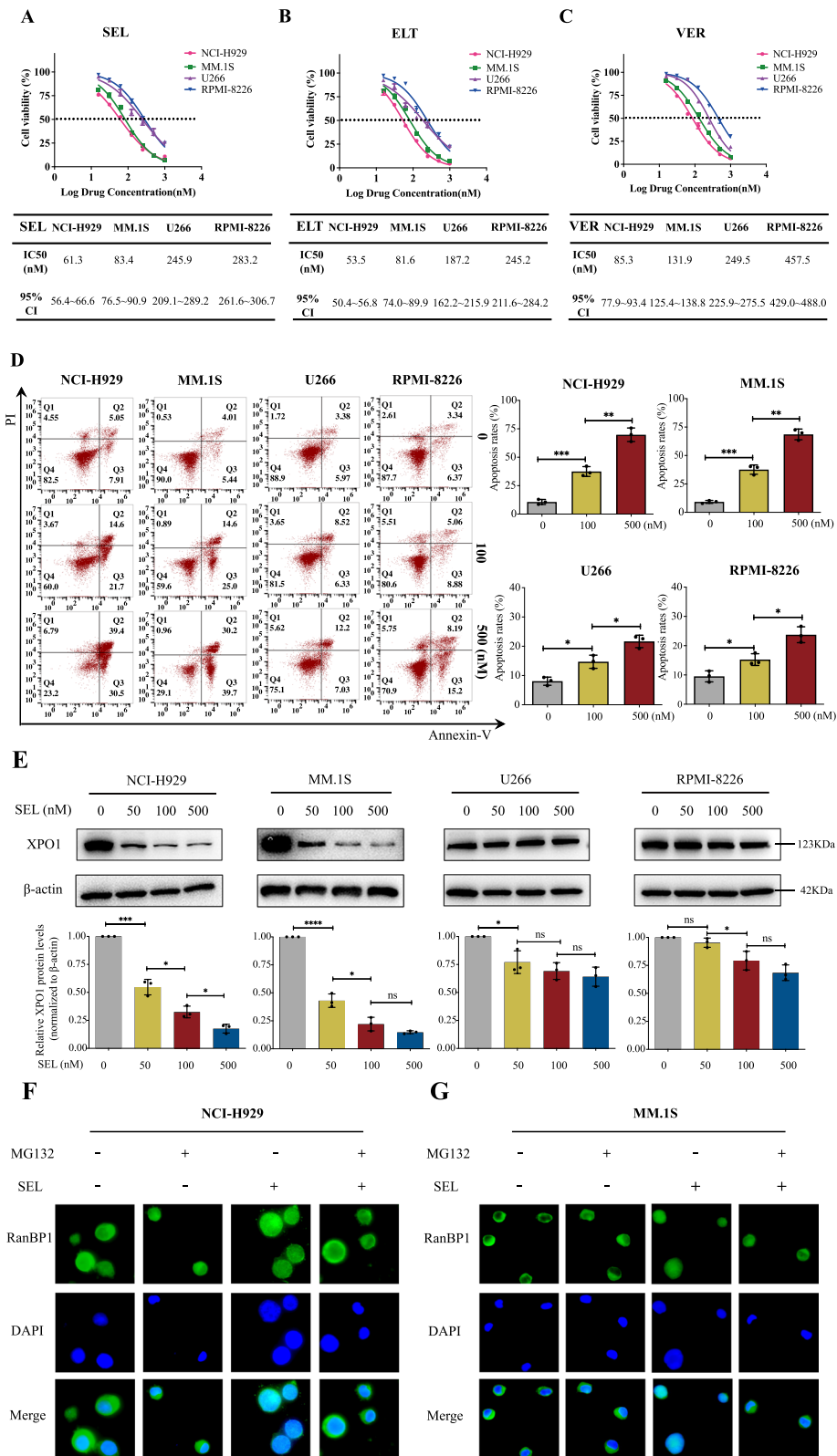


Fig. 2 (See legend on previous page.)

USP7 is the target responsible for SEL-induced degradation of XPO1

The above results clearly indicate that SEL reduces XPO1 protein levels by promoting its ubiquitination and degradation, which is crucial for the functional inhibition of XPO1 by SEL. Due to the increased ubiquitination of XPO1 induced by SEL, we speculate that there may be either an increased interaction of a specific E3 ligase with XPO1 or a decreased interaction of a particular deubiquitinating enzyme with XPO1. To identify potential inducers of XPO1 ubiquitination upon SEL treatment in MM cells, we conducted Co-IP assays to isolate XPO1-interacting proteins from both SEL-treated and control cells. The co-immunoprecipitated proteins were separated using SDS-PAGE and subsequently stained with Coomassie Brilliant Blue (Fig. 3A). Preliminary observations indicate a noticeable difference between the two sets of protein bands in the two groups, particularly noting a significant reduction in proteins around 130 kDa in the SEL-treated group. After IP-MS detection and subsequent analysis, a total of 313 interacting proteins were identified in the control group, and 462 interacting proteins were identified in the SEL-treated group (Fig. 3D). UbiBrowser 2.0 database was additionally employed to predict the potential ubiquitin ligases (Fig. 3B) and deubiquitinases (Fig. 3C) of XPO1 with high confidence. As mentioned above, potential targets include: (1) deubiquitinases that interact with XPO1 in the control group but lose this interaction in the SEL-treated group; and (2) ubiquitin ligases that do not bind to XPO1 in the control group but do establish binding with XPO1 in the SEL-treated group. By integrating IP-MS and UbiBrowser prediction results, deubiquitinase USP7 emerged as the sole candidate meeting the screening criteria, characterized by a reduced binding affinity with XPO1 following SEL treatment (Fig. 3D). Hence, USP7 was identified as a candidate for SEL-induced XPO1 degradation and selected for further validation. Using Co-IP assay, we confirmed that USP7 possesses an endogenous interaction with XPO1 in NCI-H929 and MM.1S cells (Fig. 3E, F), while SEL substantially disrupts this interaction (Fig. 3G).

These results indicate that USP7 is a potential deubiquitinating enzyme of XPO1, and SEL promotes the degradation of XPO1 by inhibiting the interaction between USP7 and XPO1.

USP7 deubiquitinates and stabilizes XPO1 in MM cells

To elucidate the role of USP7 in maintaining the stability of the XPO1 protein, we subsequently developed two doxycycline-inducible shRNA constructs (#1 and #2) targeting human USP7 for transduction into MM cells. 1 µg/mL DOX was added to the culture medium to induce the silencing of USP7. After 48 h, the knockdown efficiency was validated at both mRNA (Supplementary Fig. S2) and protein levels (Fig. 4A, B). We also assessed the expression levels of XPO1 in NCI-H929 and MM.1S cells after the knockdown of USP7. As illustrated in Fig. 4C, D, the downregulation of USP7 in MM cells resulted in a significant decrease in XPO1 protein levels, while XPO1 mRNA levels remained largely unchanged. Using the CHX-chase assay, we further confirmed that the half-life of XPO1 was significantly decreased when USP7 was depleted in MM cells (Fig. 4E). Subsequently, we investigated the potential impact of USP7 on the ubiquitination of XPO1. As shown in Fig. 4F, knockdown of USP7 led to a notable increase in the ubiquitination level of endogenous XPO1 in MM cells. Based on these findings, we conclude that USP7 stabilizes XPO1 protein through its deubiquitinating activity.

USP7 expression is elevated in SEL-insensitive MM cell lines and correlated with poorer survival in MM patients

Given that USP7 is the primary target for SEL-induced degradation of XPO1, we further explored the potential impact of USP7 expression on the therapeutic efficacy of SEL. We examined the expression levels of USP7 in both SEL-sensitive and SEL-insensitive cells. By analyzing mRNA expression data from the Human Protein Atlas (HPA) database, we found that USP7 expression was much lower in cells exhibiting greater sensitivity to SEL (Fig. 5A). We also conducted in vitro assays to validate the above results. As shown in Fig. 5B, C, the relative

(See figure on next page.)

Fig. 3 USP7 is the target responsible for SEL induced degradation of XPO1. **A** Coomassie blue staining of SDS gel loaded with proteins immunoprecipitated using anti-XPO1 antibodies from DMSO treated or 500 nM SEL treated NCI-H929 cells. The red arrow indicates the position corresponding to the molecular weight of USP7, the green arrow denotes the position for the molecular weight of XPO1. **B** and **C** UbiBrowser was employed to explore the potential ubiquitin ligases (**B**) and deubiquitinases (**C**) that may interact with XPO1. **D** The Venn diagram illustrates the overlap between the XPO1 interacting proteins identified by IP-MS and the prediction results obtained from UbiBrowser. **E** and **F** Representative immunoblotting images of Co-IP assays reveal that endogenous USP7 interacts with XPO1 in NCI-H929 and MM.1S cells. **G** NCI-H929 cells were treated with DMSO or 500 nM SEL for 4 h, then cell lysates were prepared for Co-IP assays, 1 µg of the anti-bait protein antibody was added to each group, representative immunoblotting images and the quantitative analysis results demonstrated that SEL impaired the interaction between USP7 and XPO1. The data are expressed as mean ± SD. * $p < 0.05$, ** $p < 0.01$, *** $p < 0.001$, and **** $p < 0.0001$

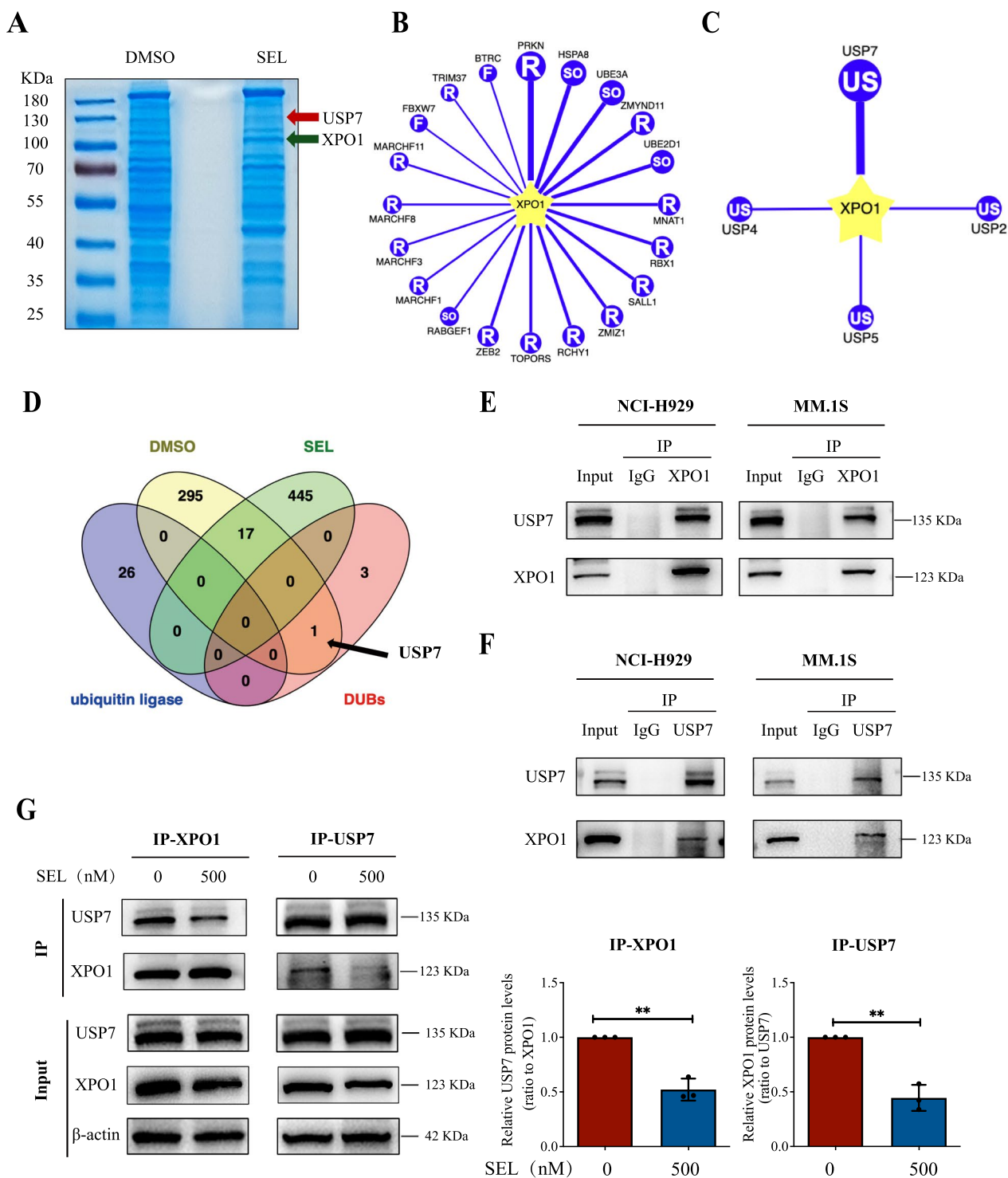


Fig. 3 (See legend on previous page.)

expression levels of USP7 mRNA and protein in U266 and RPMI-8226 cells were significantly higher compared to those in NCI-H929 and MM.1S cells. Furthermore, we performed a correlation analysis, which revealed a

positive correlation between the protein expression levels of USP7 and XPO1 in MM cell lines (Fig. 5D). These findings indicate that elevated USP7 expression is associated with decreased sensitivity to SEL. To explore the

(See figure on next page.)

Fig. 4 USP7 deubiquitinates and stabilizes XPO1 protein in MM cells. **A–D** NCI-H929 and MM.1S cells were transfected with the tet-on-shRNA either with control sequence (NC) or sequences targeting USP7 (#1 and #2), cells were treated with 1 μ g/ml DOX for 48 h, USP7 (**A** and **B**) and XPO1 (**A** and **C**) protein levels were analyzed by immunoblotting and were quantitatively analyzed. XPO1 mRNA (**D**) levels were analyzed by RT-qPCR. **E** NCI-H929 cells were transfected with indicated tet-on-shRNA, then cells were treated with 200 μ g/ml CHX for specified durations, XPO1 protein levels were assessed by immunoblotting and were quantitatively analyzed. **F** NCI-H929 cells were transfected with indicated tet-on-shRNA, cells were treated with 10 μ M MG132 for 6 h prior to collection, then XPO1 were immunoprecipitated with anti-XPO1 antibody, ubiquitination levels of endogenous XPO1 protein were analyzed by immunoblotting using the ubiquitin antibody. The data are expressed as mean \pm SD. * p <0.05, ** p <0.01, *** p <0.001, and **** p <0.0001

potential implications of targeting USP7 for the treatment of MM, we analyzed the relationship between USP7 expression and prognosis of MM patients. As shown in Fig. 5E, elevated levels of USP7 were associated with shorter overall survival (OS) in patients with MM across CoMMpass, GSE24080 as well as GSE2658 cohorts. These results highlight the potential value of targeting USP7 to enhance the therapeutic efficacy of SEL in MM treatment.

Targeting USP7 potentiates the cytotoxic effects of SEL in MM cells in vitro

To evaluate whether inhibition of USP7 could enhance the sensitivity of MM cells to SEL, we conducted further experimental analysis. We transduced tet-on-shUSP7 (#1) into the two relatively resistant cell lines, including U266 and RPMI-8226 cells. The USP7 expression levels were validated at protein levels (Fig. 6A). Subsequently, we evaluated cytotoxic effects of SEL in these cells under different conditions. As shown in Fig. 6B, knockdown of USP7 significantly enhanced the cell growth inhibition induced by SEL. Additionally, SEL-induced apoptosis rates were also significantly increased upon USP7 knockdown (Fig. 6C).

To explore whether pharmacological inhibition of USP7 could mimic the effects observed with genetic knockdown, we combined SEL with the small molecule USP7 inhibitor P5091. We found that P5091 significantly enhanced SEL-induced cell growth inhibition in those insensitive cell lines (Fig. 6D). To further validate the clinical significance of our findings, we assessed the efficacy of the combination of P5091 and SEL in primary CD138⁺ cells isolated from MM patients. The cell viability analysis showed that the combination treatment was more effective in inhibiting cell proliferation than either agent administered alone (Fig. 6E). Collectively, these results suggest that the inhibition of USP7 can enhance SEL-induced cell death in MM cells.

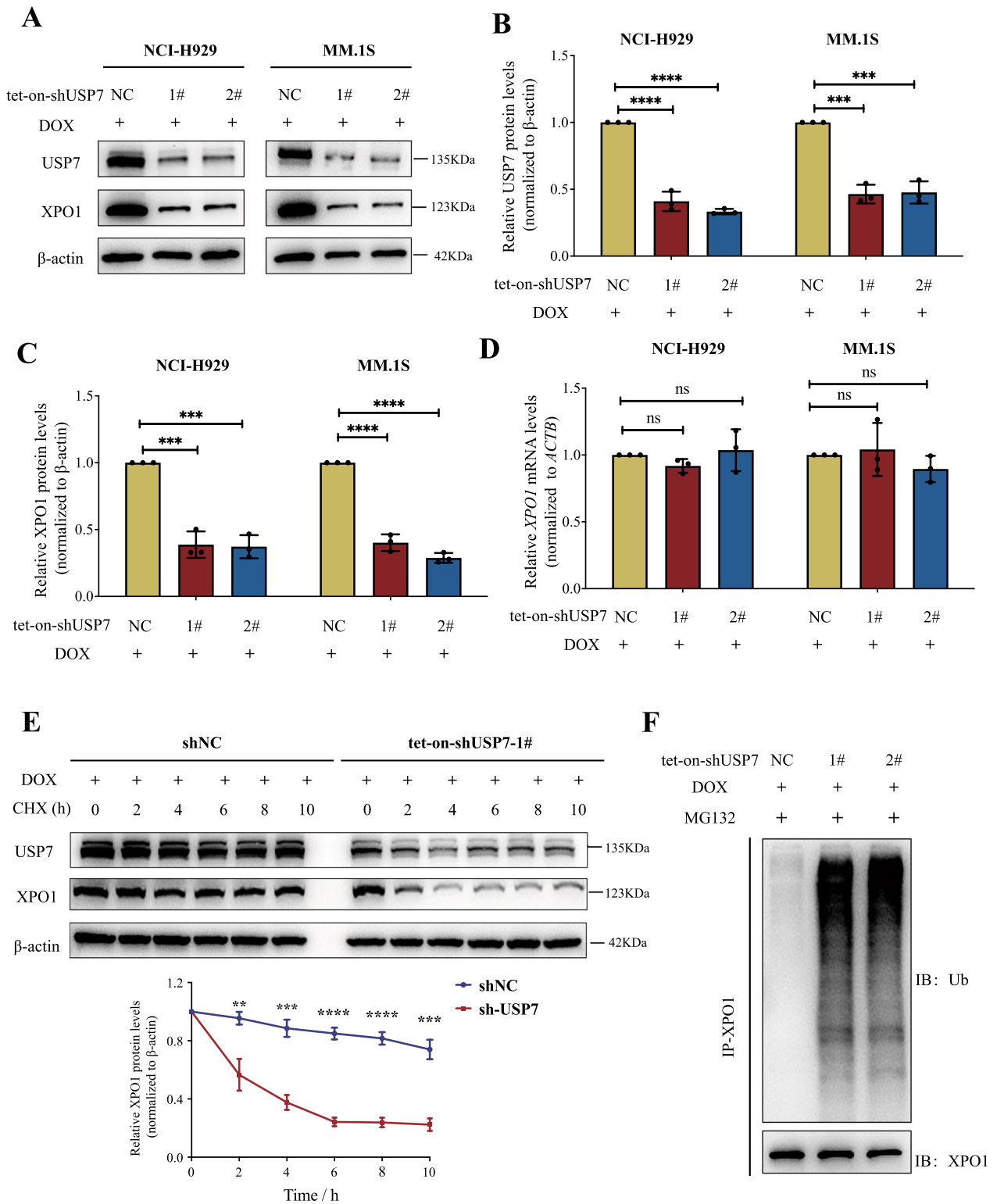
Knockdown of USP7 enhances the sensitivity of MM to SEL in vivo

To provide in-vivo evidence that USP7 inhibition could enhance the therapeutic efficacy of SEL in MM, we subcutaneously injected tet-on-shUSP7 U266 cells into NOD-SCID mice. When the tumors became palpable, we treated them with control diluents, DOX (0.25 mg/mL), SEL (10 mg/Kg), or the combination of DOX and SEL (Fig. 7A). We evaluated the tumor sizes in different groups to investigate the effect of USP7 knockdown on sensitivity to SEL. As shown in Fig. 7B–D, while single SEL treatment had a moderate effect on tumor growth, the combination of USP7 silencing with SEL led to significant tumor growth inhibition. In addition, immunohistochemical staining showed a significant decrease in the expression of the proliferation marker Ki-67 in the combination inhibition group (Fig. 7E). Collectively, these findings suggest that targeting USP7 could represent a promising therapeutic approach for enhancing the therapeutic efficacy of SEL in MM.

Discussion

Although considerable advancements have been achieved in the treatment of myeloma, most patients ultimately develop relapsed or refractory disease [23]. The nuclear export system is a promising target for anticancer therapy [24]. Targeting XPO1 with SINE compounds, such as SEL, forces the nuclear retention and functional activation of TSPs and growth regulators, thereby inducing cancer cell apoptosis and cell cycle arrest [25, 26]. The clinical benefit of SEL has been investigated in numerous clinical trials, and the results showed that therapeutic responses of SEL differ largely among MM patients [27, 28]. Inherent and acquired resistance present a significant challenge. A deeper analysis of molecular mechanisms underlying the anti-myeloma effects of SEL as well as factors that affect drug sensitivity is crucial for improving therapeutic efficacy of SEL-based treatments.

Previous studies have reported that SEL inhibit nuclear export of cargo proteins by directly disrupting their



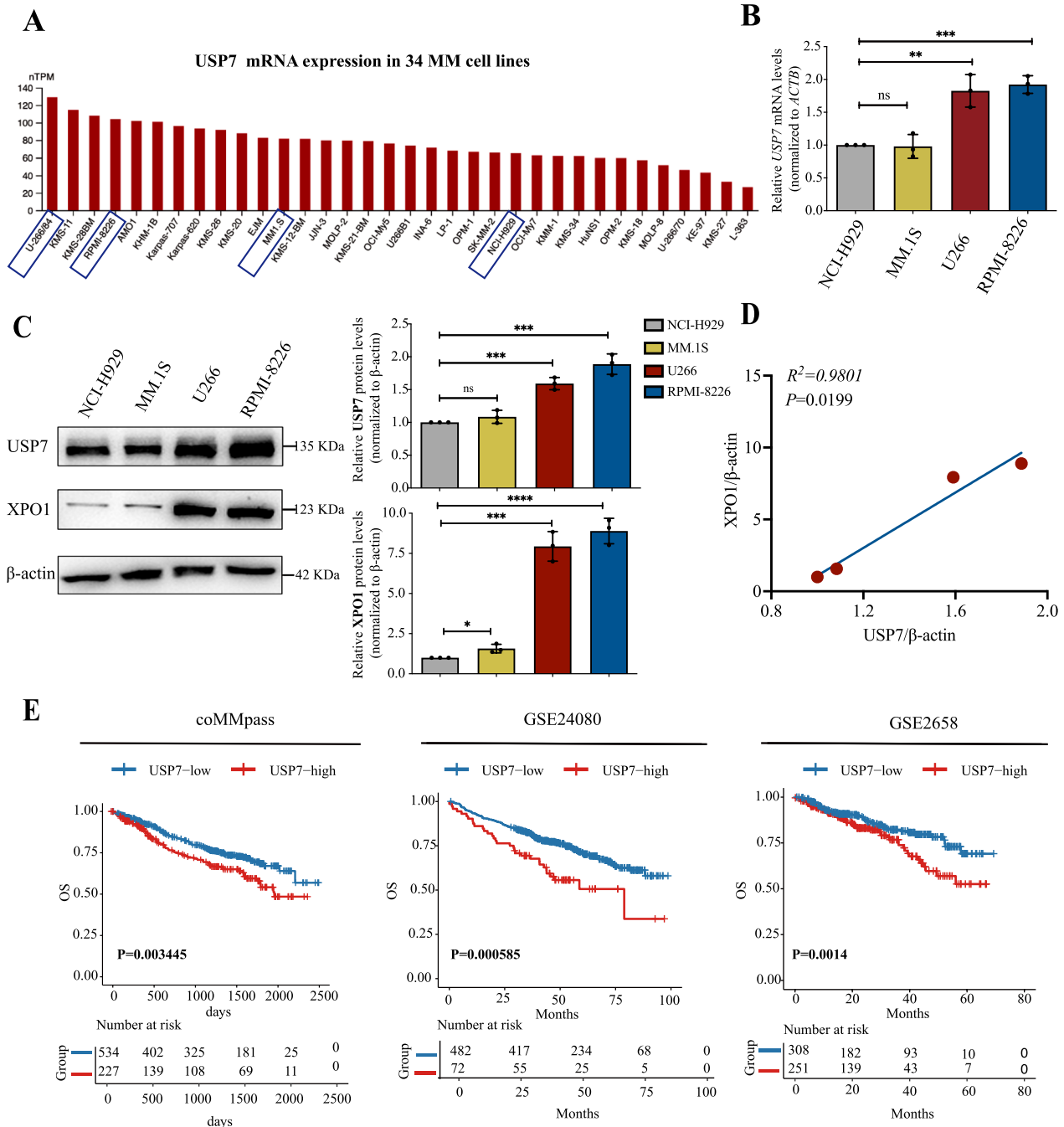


Fig. 5 USP7 expression is elevated in SEL-insensitive MM cell lines and correlated with poorer survival in MM patients. **A** USP7 mRNA expression in 34 different MM cell lines from Human Protein Atlas Database. **B** RT-qPCR analysis of USP7 mRNA levels in MM cell lines with varying sensitivity to SEL. **C** Representative western blot image of USP7 and XPO1 protein levels in MM cell lines and the quantitative analysis results. **D** Correlational analysis of XPO1 and USP7 protein levels in different MM cell lines. **E** The Kaplan–Meier analysis showed that higher USP7 expression in MM patients correlated with shorter OS in coMMpass (n = 761), GSE24080 (n = 554) and GSE2658 (n = 559) cohorts. The data are expressed as mean \pm SD. * $p < 0.05$, ** $p < 0.01$, *** $p < 0.001$, and **** $p < 0.0001$

binding to XPO1 [29]. In addition, SEL can induce XPO1 protein degradation in live cells [30]. It is still not clear whether SEL needs to reduce XPO1 protein levels to

impair its function. To gain a comprehensive understanding of the pharmacological mechanisms of SEL, we investigated the role of XPO1 degradation in the anti-myeloma

effects of SEL, as well as the underlying mechanisms of SEL-induced degradation of XPO1.

To investigate the significance of XPO1 degradation in the effectiveness of SEL, we first compared the differences in XPO1 degradation across MM cells with varying sensitivities to SEL. In addition, we analyzed the alterations in cargo nuclear export before and after blocking XPO1 degradation. We observed that the downregulation of XPO1 protein upon SEL treatment is particularly more pronounced in sensitive cells. Furthermore, inhibition of XPO1 degradation attenuates the suppressive effect of SEL on the nuclear export of cargo. Based on these results, we established the essential role of XPO1 degradation in mediating the anti-myeloma efficacy of SEL. Furthermore, we evaluated the binding capacity of various cargo molecules to XPO1 following SEL treatment (data not shown). We were surprised to find that SEL did not impair the binding of $\text{I}\kappa\text{B-}\alpha$ to XPO1, despite $\text{I}\kappa\text{B-}\alpha$ has been confirmed to confer the anti-myeloma effects of SEL [10]. This phenomenon may be explained by the considerable diversity in the NESs of different cargo proteins, both in terms of their sequences and the structures they adopt when bound to XPO1. NESs are best described by a set of six consensus sequences, which differ in the spacings between four key hydrophobic residues $\Phi 1$, $\Phi 2$, $\Phi 3$, and $\Phi 4$. NES usually has 4–5 hydrophobic residues that bind hydrophobic pockets in a hydrophobic groove of XPO1. Recent studies have found that a type of all-helix nuclear localization signal bind exclusively to the minor NES-binding site of XPO1, like *cdc7* and *midia2* [31]. XPO1 inhibitors bind into the NES-binding cleft of XPO1 to cover hydrophobic groove of XPO1 thus to prevent the formation of XPO1/cargo complexes. Different inhibitors occupy different extents of the invariant NES-binding groove. KPT compounds binds to XPO1 through the Cys528 site, which is located between the $\Phi 3$ and $\Phi 4$ pockets. While drugs like leptomycin B (LMB) occupies almost all Φ pockets, the KPT compounds only occupy a small part of the NES-binding groove [32]. This may partially explain why LMB are more toxic than other inhibitors. Further studies are still needed to explore the suppression spectrum of different inhibitors. Nevertheless, our

study confirmed the pivotal role of XPO1 degradation in the anti-myeloma effects of SEL and provided important clues for factors that affect SEL efficacy.

As mentioned above, although several previous studies have reported that SEL can induce XPO1 degradation, the underlying molecular mechanisms remain incompletely explored. Using CRISPR-Cas genome editing technology, Kwanten et al. identified E3 ubiquitin ligase ASB8 as a potential molecule affecting SEL sensitivity [17]. However, functional experiments in their study failed to provide additional support for the relationship between ASB8 expression and sensitivity to SEL. Considering that the ubiquitination levels of proteins are usually regulated by a variety of ubiquitin-modulating molecules, this indicates that additional mechanisms may also be involved. Therefore, we employed alternative experimental methods for exploration. Using IP-MS detection, we compared the differences in XPO1 interacting proteins before and after SEL treatment. We focused on ubiquitin ligase and deubiquitinating enzyme molecules and found deubiquitinating enzymes USP7 was the only target met the selection criteria. Through a series of biological experiments, we demonstrated that USP7 enhances the stability of the XPO1 protein through its deubiquitinating activity, while SEL promotes the degradation of XPO1 by disrupting the direct interaction between USP7 and XPO1 (Fig. 8). Additionally, through in vivo and in vitro experiments, we validated the impact of USP7 expression on SEL sensitivity.

USP7, also known as Ubiquitin-specific protease 7, is an enzyme that plays a crucial role in the regulation of protein degradation and cellular signaling by removing ubiquitin molecules from target proteins [33]. USP7 is involved in various biological processes, including cell cycle regulation, DNA repair, and the response to stress [34, 35]. Previous studies have confirmed the essential role of USP7 in the progression and drug resistance in MM [36, 37]. Through our research, we also demonstrated the regulatory effects of USP7 in the response to SEL treatment, thereby providing experimental evidence for the development of novel combination therapeutic strategies.

(See figure on next page.)

Fig. 6 Targeting USP7 potentiates the cytotoxic effects of SEL in MM cells in vitro. **A–C** U266 and RPMI-8226 cells were transfected with tet-on-shUSP7(#1), USP7 protein expression following DOX treatment were detected by western blotting and were quantitatively analyzed (**A**). Cell viability of the cells treated with indicated drugs were detected by CCK8 assays (**B**). Apoptosis of MM cells treated with indicated drugs were detected by flow cytometry following staining with Annexin-V/PI (**C**). **D** and **E** U266, RPMI-8226 cell lines (**D**) and primary MM cells (**E**) were treated with 100 nM SEL and/or 5 μM P5091 for 48 h. Cell viability was detected by CCK8. The data are expressed as mean \pm SD. * $p < 0.05$, ** $p < 0.01$, *** $p < 0.001$, and **** $p < 0.0001$

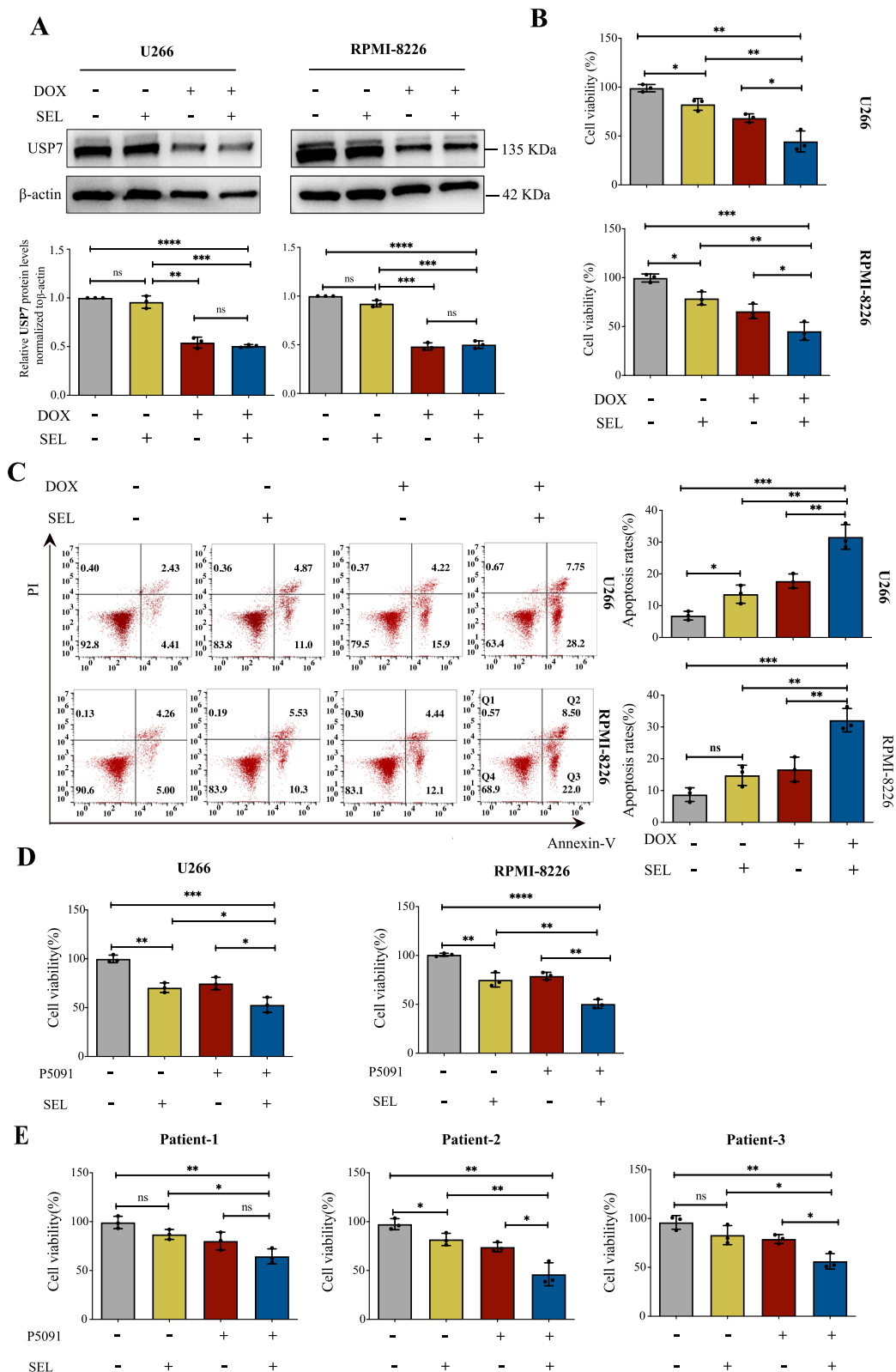


Fig. 6 (See legend on previous page.)

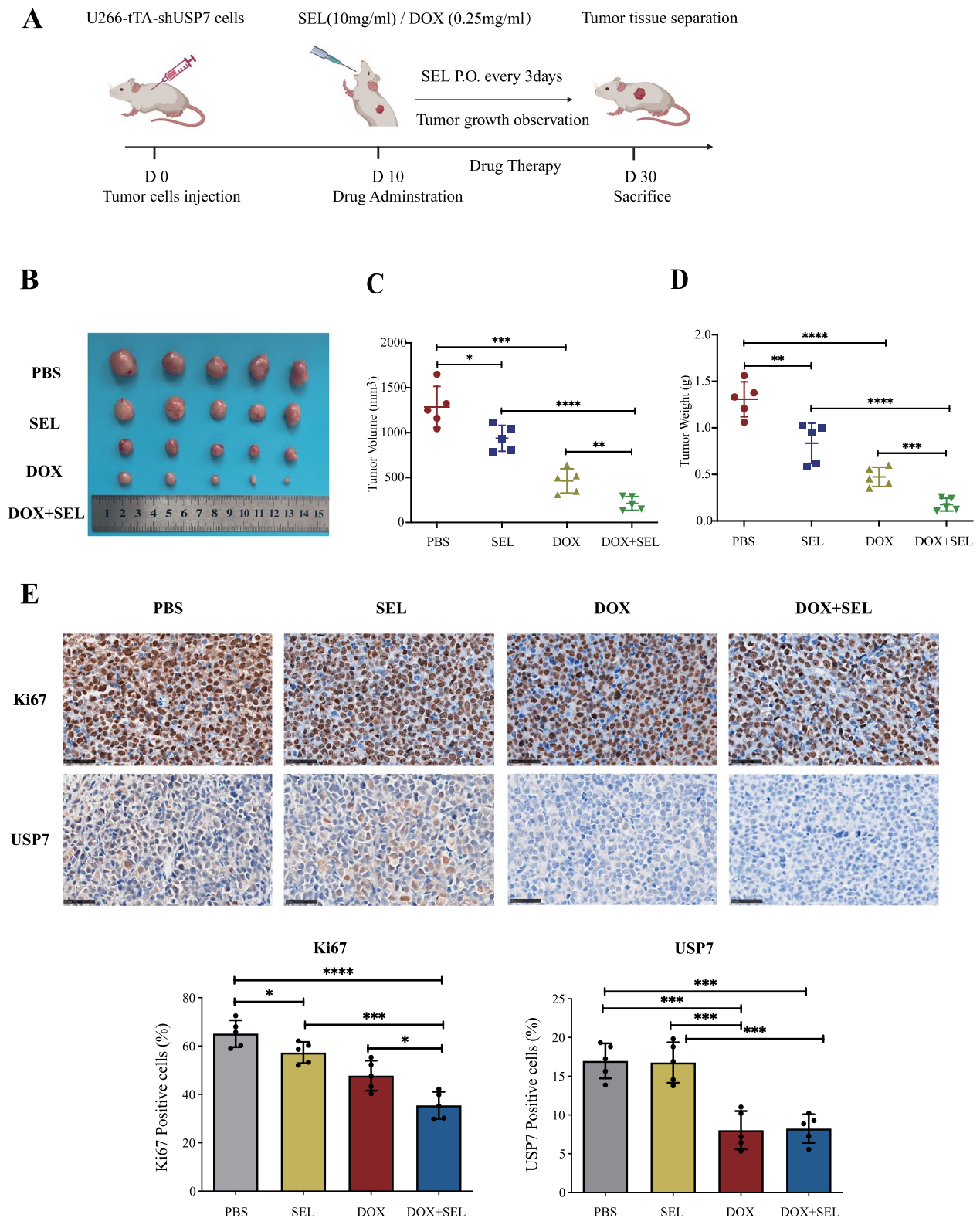


Fig. 7 Knockdown of USP7 enhances the sensitivity of MM to SEL in vivo. **A** Procedure for animal experiments (n = 20, n = 5/group). The graphic was generated using Biorender. **B** Photographic images of xenografts in NOD-SCID mice of each group. **C** Quantitative analysis of tumor volume in the different groups. **D** Quantitative analysis of tumor weights in the different groups. **E** Immunohistochemical staining of Ki-67 and USP7 in the xenograft tumor tissues, and the quantitative analysis results of the proportion of positive cells. Data are shown as mean ± SD. **p* < 0.05, ***p* < 0.01, ****p* < 0.001, *****p* < 0.0001

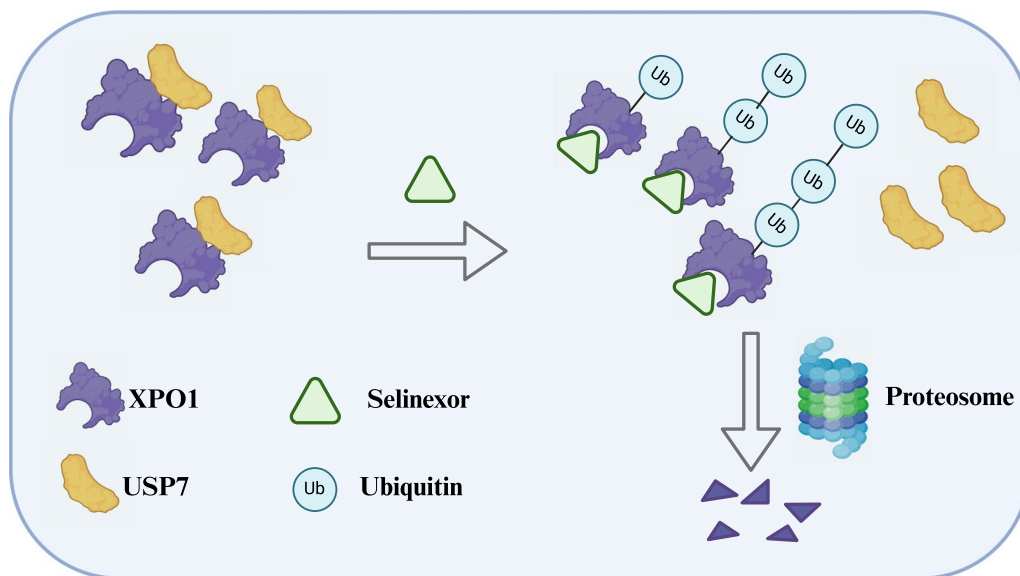


Fig. 8 Schematic showing the mechanism of SEL-induced XPO1 degradation in MM cells: SEL disrupts the interaction between XPO1 and USP7, leading to the ubiquitination and subsequent degradation of XPO1. The graphic was created using Biorender

Conclusions

In summary, our study demonstrated for the first time the role of XPO1 degradation in the anti-myeloma activity of SEL and elucidated the underlying mechanism of SEL induced ubiquitination of XPO1 protein. Besides, we clarified the molecular biological function of USP7 in maintaining XPO1 stabilization and mediating SEL resistance. Our results may help to provide new clues for improving the therapeutic efficiency of SEL-based treatment in myeloma.

Abbreviations

CHX	Cycloheximide
ELT	Eltanexor
IP-MS	Immunoprecipitation-mass spectrometry
IC50	Half inhibitory concentration
LMB	Leptomycin B
MM	Multiple Myeloma
NES	Nuclear export signal
PI	Propidium iodide
RRMM	Relapsed/Refractory MM
SEL	Selinexor
SINE	Selective inhibitors of nuclear export
SDS-PAGE	Sulfate-polyacrylamide gel electrophoresis
shRNA	Short hairpin RNA
TSPs	Tumor suppressor proteins
VER	Verdinexor
XPO1	Exportin1

Supplementary Information

The online version contains supplementary material available at <https://doi.org/10.1186/s12967-025-06068-3>.

Additional file 1.

Acknowledgements

We are grateful to the proteome platform of the institute of human phenotypes at Fudan University for their support of this study.

Author contributions

JW conducted the experiments and drafted the manuscript. MC performed bioinformatics analysis. JJ collected the bone marrow samples. YW and XL provided technical or material support. MZ, FX, LZ, and HZ have reviewed and edited the manuscript. ZQ conducted IP-MS detection. JH designed the study. All authors reviewed and approved the final manuscript.

Funding

This work was supported by the National Natural Science Foundation of China (81974006), and Shanghai Shenkang Hospital Development Center Funding (SHDC2020CR2070B).

Data availability

The datasets analysed in the current study are available in the Human Protein Atlas (<https://www.proteinatlas.org>) and Ubibrowser^{2.0} databases (http://ubibrowser.bio-it.cn/ubibrowser_v3/). The mass spectrometry detection results in the current study are available from the corresponding author on reasonable request.

Declarations

Ethics approval and consent to participate

This study was approved by the ethics committee of Ren Ji Hospital, Shanghai Jiao Tong University School of Medicine (Ethics Approval Number: KY2020-191).

Consent for publication

All the authors have declared that they agree to publish.

Competing interests

The authors declared no competing interest.

Author details

¹Department of Hematology, Ren Ji Hospital, Shanghai Jiao Tong University School of Medicine, Shanghai 200127, China. ²Department of Hematology, Punan Hospital of Pudong New District, Shanghai 200125, China. ³Key Laboratory of Genetic Engineering and Collaborative Innovation Center for Genetics and Development, School of Life Sciences, Institute of Biomedical Sciences, Human Phenome Institute, Zhongshan Hospital, Fudan University, Shanghai 200433, China.

Received: 15 November 2024 Accepted: 5 January 2025

Published online: 13 January 2025

References

- Cowan AJ, Green DJ, Kwok M, et al. Diagnosis and management of multiple myeloma: a review. *JAMA*. 2022;327(5):464–77.
- Rodriguez-Otero P, Paiva B, San-Miguel JF. Roadmap to cure multiple myeloma. *Cancer Treat Rev*. 2021;100: 102284.
- Rajkumar SV, Kumar S. Multiple myeloma current treatment algorithms. *Blood Cancer J*. 2020;10(9):94.
- Azmi AS, Uddin MH, Mohammad RM. The nuclear export protein XPO1— from biology to targeted therapy. *Nat Rev Clin Oncol*. 2021;18(3):152–69.
- Wickramasinghe VO, Laskey RA. Control of mammalian gene expression by selective mRNA export. *Nat Rev Mol Cell Biol*. 2015;16(7):431–42.
- Volpon L, Culjkovic-Kraljacic B, Sohn HS, et al. A biochemical framework for eIF4E-dependent mRNA export and nuclear recycling of the export machinery. *RNA (New York, NY)*. 2017;23(6):927–37.
- Camus V, Miloudi H, Taly A, et al. XPO1 in B cell hematological malignancies: from recurrent somatic mutations to targeted therapy. *J Hematol Oncol*. 2017;10(1):47.
- Taylor J, Sendino M, Gorelick AN, et al. Altered nuclear export signal recognition as a driver of oncogenesis. *Cancer Discov*. 2019;9(10):1452–67.
- Turner JG, Dawson JL, Grant S, et al. Treatment of acquired drug resistance in multiple myeloma by combination therapy with XPO1 and topoisomerase II inhibitors. *J Hematol Oncol*. 2016;9(1):73.
- Turner JG, Kashyap T, Dawson JL, et al. XPO1 inhibitor combination therapy with bortezomib or carfilzomib induces nuclear localization of IκBα and overcomes acquired proteasome inhibitor resistance in human multiple myeloma. *Oncotarget*. 2016;7(48):78896–909.
- Azizian NG, Li Y. XPO1-dependent nuclear export as a target for cancer therapy. *J Hematol Oncol*. 2020;13(1):61.
- Richard S, Richter J, Jagannath S. Selinexor: a first-in-class SINE compound for treatment of relapsed/refractory multiple myeloma. *Future Oncol*. 2020;16(19):1331–50.
- Grosicki S, Simonova M, Spicka I, et al. Once-per-week selinexor, bortezomib, and dexamethasone versus twice-per-week bortezomib and dexamethasone in patients with multiple myeloma (BOSTON): a randomised, open-label, phase 3 trial. *Lancet*. 2020;396(10262):1563–73.
- Qiu L, Xia Z, Fu C, et al. Selinexor plus low-dose dexamethasone in Chinese patients with relapsed/refractory multiple myeloma previously treated with an immunomodulatory agent and a proteasome inhibitor (MARCH): a phase II, single-arm study. *BMC Med*. 2022;20(1):108.
- Hing ZA, Fung HY, Ranganathan P, et al. Next-generation XPO1 inhibitor shows improved efficacy and in vivo tolerability in hematological malignancies. *Leukemia*. 2016;30(12):2364–72.
- Conforti F, Zhang X, Rao G, et al. Therapeutic effects of XPO1 inhibition in thymic epithelial tumors. *Cancer Res*. 2017;77(20):5614–27.
- Kwanten B, Deconick T, Walker C, et al. E3 ubiquitin ligase ASB8 promotes selinexor-induced proteasomal degradation of XPO1. *Biomed Pharmacother*. 2023;160: 114305.
- Chen K, Cheng HH, Zhou RJ. Molecular mechanisms and functions of autophagy and the ubiquitin-proteasome pathway. *Yi Chuan*. 2012;34(1):5–18.
- Li S, Fu J, Walker CJ, et al. Dual targeting of protein translation and nuclear protein export results in enhanced antimyeloma effects. *Blood Adv*. 2023;7(12):2926–37.
- Hu F, Chen XQ, Li XP, et al. Drug resistance biomarker ABCC4 of selinexor and immune feature in multiple myeloma. *Int Immunopharmacol*. 2022;108: 108722.
- Li Y, Zhou J, Min S, et al. Distinct RanBP1 nuclear export and cargo dissociation mechanisms between fungi and animals. *Elife*. 2019;8: e41331.
- Saito N, Sakakibara K, Sato T, et al. CBS9106-induced CRM1 degradation is mediated by cullin ring ligase activity and the neddylation pathway. *Mol Cancer Ther*. 2014;13(12):3013–23.
- Pinto V, Bergantim R, Cairns HR, et al. Multiple myeloma: available therapies and causes of drug resistance. *Cancers (Basel)*. 2020;12(2):407.
- Garfall AL. New biological therapies for multiple myeloma. *Annu Rev Med*. 2024;75:13–29.
- Benkova K, Mihalyova J, Hajek R, et al. Selinexor, selective inhibitor of nuclear export: unselective bullet for blood cancers. *Blood Rev*. 2021;46: 100758.
- Liu S, Qiao W, Sun Q, et al. Chromosome region maintenance 1 (XPO1/CRM1) as an anticancer target and discovery of its inhibitor. *J Med Chem*. 2021;64(21):15534–48.
- Cornell R, Hari P, Tang S, et al. Overall survival of patients with triple-class refractory multiple myeloma treated with selinexor plus dexamethasone vs standard of care in MAMMOTH. *Am J Hematol*. 2021;96(1):E5–e8.
- Delimpasi S, Mateos MV, Auner HW, et al. Efficacy and tolerability of once-weekly selinexor, bortezomib, and dexamethasone in comparison with standard twice-weekly bortezomib and dexamethasone in previously treated multiple myeloma with renal impairment: Subgroup analysis from the BOSTON study. *Am J Hematol*. 2022;97(3):E83–6.
- Nachmias B, Schimmer AD. Targeting nuclear import and export in hematological malignancies. *Leukemia*. 2020;34(11):2875–86.
- Tai YT, Landesman Y, Acharya C, et al. CRM1 inhibition induces tumor cell cytotoxicity and impairs osteoclastogenesis in multiple myeloma: molecular mechanisms and therapeutic implications. *Leukemia*. 2014;28(1):155–65.
- Fung HY, Fu SC, Chook YM. Nuclear export receptor CRM1 recognizes diverse conformations in nuclear export signals. *Elife*. 2017;6: e23961.
- Gargantilla M, López-Fernández J, Camarasa MJ, et al. Inhibition of XPO-1 mediated nuclear export through the michael-acceptor character of chalcones. *Pharmaceuticals (Basel, Switzerland)*. 2021;14(11):1131.
- Saha G, Roy S, Basu M, et al. USP7—a crucial regulator of cancer hallmarks. *Biochim Biophys Acta Rev Cancer*. 2023;1878(3): 188903.
- Valles GJ, Bezsonova I, Woodgate R, et al. USP7 is a master regulator of genome stability. *Front Cell Dev Biol*. 2020;8:717.
- Carreira LD, Oliveira RI, Moreira VM, et al. Ubiquitin-specific protease 7 (USP7): an emerging drug target for cancer treatment. *Expert Opin Ther Targets*. 2023;27(11):1043–58.
- Li C, Xia J, Franqui-Machin R, et al. TRIP13 modulates protein deubiquitination and accelerates tumor development and progression of B cell malignancies. *J Clin Invest*. 2021;131(14): e146893.
- Tang P, Yu Z, Sun H, et al. CRIP1 involves the pathogenesis of multiple myeloma via dual-regulation of proteasome and autophagy. *EBioMedicine*. 2024;100: 104961.

Publisher's Note

Springer Nature remains neutral with regard to jurisdictional claims in published maps and institutional affiliations.